Hydrodynamics of an endothermic gas with application to bubble cavitation

James F. Lutsko[a)]
Center for Nonlinear Phenomena and Complex Systems, Université Libre de Bruxelles,
C.P. 231, Boulevard du Triomphe, 1050 Brussels, Belgium

The hydrodynamics for a gas of hard spheres which sometimes experience inelastic collisions resulting in the loss of a fixed, velocity-independent, amount of energy Δ is investigated with the goal of understanding the coupling between hydrodynamics and endothermic chemistry. The homogeneous cooling state of a uniform system and the modified Navier-Stokes equations are discussed and explicit expressions given for the pressure, cooling rates, and all transport coefficients for D dimensions. The Navier-Stokes equations are solved numerically for the case of a two-dimensional gas subject to a circular piston so as to illustrate the effects of the enegy loss on the structure of shocks found in cavitating bubbles. It is found that the maximal temperature achieved is a sensitive function of Δ with a minimum occurring near the physically important value of $\Delta \sim 12\,000$ K ~ 1 eV. © *2006 American Institute of Physics.* [DOI: 10.1063/1.2357150]

I. INTRODUCTION

Sonochemistry allows for the achievement of extreme temperatures, pressures, and densities in simple, tabletop experiments.[1] This is because ultrasound excites bubble cavitation which in turn gives rise to these extreme conditions. The results are important both because bubble cavitation occurs naturally[2] and because of the theoretical and technological interest in both bubble cavitation and ultrasound technology.[1,3] One of the most well-known manifestations of sonochemistry is sonoluminescence whereby, under certain conditions, fluids irradiated with ultrasound are observed to emit light.[3] The conversion of mechanical energy into electromagnetic form occurs at the high temperatures and pressures achieved during bubble cavitation, although many details such as the composition of the gases inside the bubbles and the relative importance of various light-generating mechanisms remain unclear. Many recent theoretical studies have focused on modeling the behavior of a single gas bubble embedded in a liquid and subjected to sound waves.[4–9] The predicted temperatures achieved at the points of maximum compression are typically of the order $10^4 - 10^5$ K and shocks are sometimes observed to form although their presence depends on the exact conditions of the gas and some details of the modeling. Under these extreme conditions a variety of activated chemical reactions, see, e.g., Ref. 10 collision-induced emissions,[11,12] ionization and electron-ion recombination,[13] and bremsstrahlung[14] are all expected to occur.

All of the studies cited above which take account of chemistry rely on equilibrium chemical models. The dynamics of the bubble boundary is described by the Rayleigh-Plesset equation and the chemistry by equilibrium rate equations. The bubble is either assumed to have uniform temperature, density, and pressure (called adiabatic models)

or the dynamics of the gas inside the bubble is modeled by the Navier-Stokes equations (in which case, the rate equations couple to the Navier-Stokes equations via a convective term). In all cases, the rate constants and transport coefficients used are based on the assumption that only small deviations from local equilibrium occur. However, it is not at all clear that the interior of the bubble can be adequately described by a local equilibrium ensemble, particularly when there is a significant conversion of mechanical energy (from the sound) into other, nonmechanical, forms via endothermic chemical reactions or radiation. Indeed, the experimental work of Didenko and Suslick lead them to conclude that "…the temperatures attained in single-bubble cavitation in liquids with significant vapor pressures will be substantially limited by endothermic chemical reactions of the polyatomic species inside the collapsing bubble."[15] This issue has been investigated by Yasui using an adiabatic model[10] with a similar conclusion but that work was challenged by Toegel *et al.*[16] who found that including excluded volume effects in the equation of state of the gas in an adiabatic model eliminated much of the effect. Aside from the fact that these studies ignore the gas dynamics within the bubble, there is reason to question both of these calculations as experience with granular systems has shown that even a small degree of inelasticity leads to a rich phenomenology of clustering instabilities and nonintuitive behavior[17–19] due to the inherently nonequilibrium nature of the system. This naturally leads to the question as to whether it makes any sense to ignore the nonequilibrium effects undoubtedly present during bubble cavitation.

Indeed, one could go one step further and ask whether the Navier-Stokes equations are even applicable in the presence of the large gradients predicted during cavitation. A recent comparison between the Navier-Stokes equations for a gas of hard spheres subject to a spherical compression and computer simulations of the same system did indeed give

---

a)Electronic mail: jlutsko@ulb.ac.be

125, 164319-1

support to the adequacy of the Navier-Stokes description.[20] Given this support, one must ask whether the Navier-Stokes equations plus rate equations are the correct hydrodynamic description of such systems which is properly a question which must be answered by recourse to kinetic theory. The problem here is that the only tractable kinetic theory for dense systems, and high density is an issue during bubble cavitation,[1,16] is the Enskog theory for hard spheres.[21] Fortunately, hard spheres provide a good first approximation to the properties of real, interacting systems in all important respects including transport properties, fluid structure, and phase behavior (see, e.g., Ref. 22). The kinetic theory for chemically reactive hard spheres and the coupled hydrodynamics and reaction equations have recently been formulated and discussed[23] and at least three generic differences from the "local-equilibrium" models noted. First, even for a single species, the heat flux depends on density gradients as well as temperature gradients and a new transport coefficient must be introduced. Second, the reaction equations involve new couplings to the velocity field. Third, the cooling term—which one might introduce "by hand" into the heat equation to account for endothermic reactions—also involves new couplings to the velocity field. The first and last effects are well known for granular fluids[24] but are not normally considered in the context of cavitation.

The purpose of the present work is to investigate, within the context of a minimalist microscopic model, the role of the coupling of energy loss to hydrodynamics self-consistently, taking into account nonequilibrium effects. One result will be a richer description of the role of energy loss on the maximum temperature obtained at the center of a cavitating bubble than given in previous work.[10,16]

The detailed interaction model will be given in the next section. It consists of hard spheres which lose a fixed quantity of energy Δ upon collision, provided the rest-frame kinetic energy is sufficient. This is intended as a toy model which resembles an activated chemical process and which differs from granular fluids in the physically important sense that the energy loss is (a) discrete and (b) bounded from below—in granular fluids, a fixed fraction of the kinetic energy is lost in *all* collisions. This is not intended to model any particular radiation or chemical mechanism although it might be considered a crude model of collision-induced excitations and emission. The goal is then to derive from the kinetic theory a hydrodynamic description of the fluid using the Chapman-Enskog method.[21,23,25] Since the Chapman-Enskog method of deriving the hydrodynamic equations is basically a gradient expansion about the homogeneous fluid, the first question which must be addressed is the nature of the homogeneous state of the radiating gas. For an equilibrium hard-sphere fluid, the homogeneous system has constant temperature and the atomic velocities obey a Maxwell distribution. When inelastic collisions occur, the system loses energy continuously and the homogeneous state is not so simple: the density and temperature are spatially uniform and the macroscopic velocity field vanishes but the temperature is time dependent and the distribution of atomic velocities is no longer Maxwellian. The calculation of the cooling rate and the lowest-order corrections to the Maxwell distribution

are the subject of Sec. II of this paper. In Sec. III, the transport properties are calculated and it is shown that they behave anomalously for temperatures near the energy-loss threshold. These include the shear and bulk viscosities, the thermal conductivity, and a new transport coefficient describing the transport of heat due to density gradients. The latter is typical of interactions which do not conserve energy and plays an important role in the instabilities occurring in granular fluids. In Sec. IV, the resulting hydrodynamics is used to study the effects of the energy loss on a two-dimensional gas confined to a circular volume with contracting walls—a circular piston, which sets up shock waves within the gas. It is found that the maximum temperature obtained lowers as the energy threshold is lowered until a minimum is reached at which point the maximum temperature increases with decreasing threshold. In the final section, it is argued that the minimum may be of physical significance.

II. THE HOMOGENEOUS COOLING STATE

A. Dynamical model

Consider a collection of N hard spheres in D dimensions having diameter σ and mass m. The position and velocity of the ith particle will be denoted $\mathbf{q}_i$ and $\mathbf{v}_i$, respectively. The particles are confined to a box of volume V giving a number density $n = N/V$. The boundary conditions are not important here and could be, e.g., hard, elastic walls or periodic. The only interactions are instantaneous collisions: between collisions the particles stream freely. When two particles collide, their positions are unchanged but they lose a quantity of energy, Δ_a which could be zero. In Ref. 23 it is shown that in this case, the velocities after the collision, $\mathbf{v}_i'$ and $\mathbf{v}_j'$, will be related to the precollisional velocities, $\mathbf{v}_i$ and $\mathbf{v}_j$, by

$$\mathbf{v}_i' = \mathbf{v}_i - \frac{1}{2}\hat{q}_{ij}\left(\mathbf{v}_{ij}\cdot\hat{q}_{ij} + \text{sgn}(\mathbf{v}_{ij}\cdot\hat{q}_{ij})\sqrt{(\mathbf{v}_{ij}\cdot\hat{q}_{ij})^2 - \frac{4}{m}\Delta_a}\right),$$

$$\mathbf{v}_j' = \mathbf{v}_j + \frac{1}{2}\hat{q}_{ij}\left(\mathbf{v}_{ij}\cdot\hat{q}_{ij} + \text{sgn}(\mathbf{v}_{ij}\cdot\hat{q}_{ij})\sqrt{(\mathbf{v}_{ij}\cdot\hat{q}_{ij})^2 - \frac{4}{m}\Delta_a}\right),$$

$$\tag{1}$$

where $\hat{q}_{ij} = (\mathbf{q}_i - \mathbf{q}_j)/|\mathbf{q}_i - \mathbf{q}_j|$ is the unit vector pointing from the center of the ith particle to the center of the jth particle. This collision rule preserves the total momentum $m(\mathbf{v}_i + \mathbf{v}_j)$ as well as the total angular momentum of the colliding particles but allows for an energy loss as can be seen by computing

$$\frac{m}{2}v_i'^2 + \frac{m}{2}v_j'^2 = \frac{m}{2}v_i^2 + \frac{m}{2}v_j^2 - \Delta_a, \tag{2}$$

so that Δ_a characterizes the energy loss which may in general be any function of the normal component of the relative momentum of the colliding atoms [i.e., $\Delta_a = \Delta_a(\mathbf{v}_{ij}\cdot\hat{q}_{ij})$]. The subscript allows for the possibility that different types of collisions are possible and each collision realizes the ath collision type with probability K_a. To be specific, we will consider the simplest model of a sudden energy loss wherein for collisions with enough energy in the normal component of the momenta, i.e., $m/4(\mathbf{v}_{ij}\cdot\hat{q}_{ij})^2 > \Delta$, an inelastic collision, removing energy Δ occurs with fixed probability p and oth-

erwise the collision is elastic. In terms of the step function $\Theta(x)$ which is 0 for $x<1$ and 1 for $x>1$, this may be written as

$$K_0 = \Theta\left(\Delta - \frac{m}{4}(\mathbf{v}_{ij} \cdot \hat{q}_{ij})^2\right)$$
$$+ (1-p)\Theta\left(\frac{m}{4}(\mathbf{v}_{ij} \cdot \hat{q}_{ij})^2 - \Delta\right), \quad \Delta_0 = 0,$$
(3)

$$K_1 = p\Theta\left(\frac{m}{4}(\mathbf{v}_{ij} \cdot \hat{q}_{ij})^2 - \Delta\right), \quad \Delta_1 = \Delta,$$

where the $a=0$ collisions are elastic and the $a=1$ collisions inelastic. For $p=0$ the collisions are purely elastic and for $p=1$ the collisions are always inelastic if enough energy is available.

B. General description of the homogeneous cooling state

Given this model, for $p>0$ the system will always cool since even for very low temperatures, there will be some population of sufficiently energetic atoms which undergo inelastic collisions. Thus, the simplest state the system can experience is one which is spatially homogeneous but undergoing continual cooling, the so-called homogeneous cooling state (HCS) which is the analog of the equilibrium state for this intrinsically nonequilibrium system. In this case, the velocity distribution will not be strictly Gaussian. In fact, it has been shown[25] that the nonequilibrium velocity distribution can be written as an expansion about a simple Gaussian distribution so that

$$f_0(\mathbf{v};T(t)) = f_M(\mathbf{v};T(t)) \sum_k c_k(T(t)) L_k^{(D-2)/2}\left(\frac{m}{2k_B T(t)} v^2\right),$$
(4)

where the Maxwellian distribution for a fluid with uniform number density n and temperature T is

$$f_M(\mathbf{v};T(t)) = n\pi^{-D/2}\left(\frac{2k_B T(t)}{m}\right)^{-D/2} \exp\left(-\frac{m}{2k_B T(t)} v^2\right)$$
(5)

and the associated Laguerre polynomials are

$$L_k^{(D-2)/2}(x) = \sum_{m=0}^{k} \frac{\Gamma(D/2+k)(-x)^m}{\Gamma(D/2+m)(k-m)!m!}.$$
(6)

The temperature cools according to

$$\frac{d}{dt}T(t) = \frac{2}{Dnk_B}\xi^{(0)}$$
(7)

since the heating rate given by

$$\frac{2}{Dnk_B}\xi^{(0)} = -T\sum_{rs} I_{1,rs} c_r c_s$$
(8)

will generally be negative. The first two coefficients in the expansion of the distribution are $c_0=1$ and $c_1=0$ which fol-

low from the definition of the density and temperature.[23] The higher-order coefficients obey

$$\left(\frac{2}{Dnk_B T}\xi^{(0)}\right)\left[T\frac{\partial}{\partial T}c_k + k(c_k - c_{k-1})\right] = \sum_{rs} I_{k,rs} c_r c_s,$$
(9)

where the coefficients $I_{k,rs}$ appearing in these equations can be calculated from a generating function,[25] details of which can be found in Appendix A. It is convenient to use dimensionless variables $\Delta^* = \Delta/k_B T$, $n^* = n\sigma^D$,

$$t^* = 2p(D+2)n^*\chi\frac{S_D}{2D(D+2)\sqrt{\pi}}\left(\frac{\Delta}{m\sigma^2}\right)^{1/2} t$$
(10)

and

$$I_{k,rs} = n^*\chi\frac{S_D}{2D(D+2)\sqrt{\pi}}\left(\frac{k_B T}{m\sigma^2}\right)^{1/2} I_{k,rs}^*,$$
(11)

where the area of the unit D sphere is

$$S_D = \frac{2\pi^{D/2}}{\Gamma(D/2)}.$$
(12)

The quantity χ occurring in these expressions is the pair distribution function at contact which occurs in the Enskog theory to take account of the enhancement of the collision rate due to the finite size of the atoms. In the low-density (Boltzmann) limit, it goes to one. It is solely a function of density, and at finite densities, it is usually approximated as that of a local equilibrium fluid of hard spheres. When performing numerical calculations, the value used for two-dimensional disks will be that of the approximation by Hendersen (see, e.g., Ref. 26),

$$\chi = \frac{1 - 7y/16}{(1-y)^2}$$
(13)

with $y=\pi n\sigma^2/4$, while for three-dimensional spheres the Carnahan-Starling expression[26]

$$\chi = \frac{1 - y/2}{(1-y)^3}$$
(14)

with $y=\pi n\sigma^3/6$ will be used.

The evolution of the temperature is then given by

$$\frac{d}{dt}T(t) = -n^*\chi\frac{S_D}{2D(D+2)\sqrt{\pi}}\left(\frac{k_B T}{m\sigma^2}\right)^{1/2} T\sum_{rs} I_{1,rs}^* c_r c_s$$
(15)

or

$$\frac{d}{dt^*}\Delta^* = \frac{(\Delta^*)^{1/2}}{2p(D+2)}\sum_{rs} I_{1,rs}^* c_r c_s$$
(16)

and the coefficients of the expansion of the distribution function are

$$\frac{d}{dt^*}c_k = \frac{1}{2p(D+2)(\Delta^*)^{1/2}}$$
$$\times\left[\sum_{rs} I_{k,rs}^* c_r c_s + \left(\sum_{rs} I_{1,rs}^* c_r c_s\right)k(c_k - c_{k-1})\right],$$
(17)

here Eq. (16) has been used to replace $(d/d\Delta^*)c_k$ by $(d/dt^*)c_k$. All of these expressions are exact consequences of

the Enskog kinetic theory.[25] Generally, three approximations are made in order to solve these equations: (1) one sets $c_k = 0$ for $k > k_0$ for some integer k_0, (2) only the first k_0 equations of the coupled hierarchy given in Eq. (9) are retained, and (3) one also neglects quadratic terms $c_r c_s$ for $r+s > k_0$ and cubic terms $c_r c_s c_k$ for $r+s+k > k_0$. The first two approximations are necessary in order to make solution of the equations possible, while the third is more a matter of convenience which generally introduces no significant errors.

In the following subsections, the lowest two orders of approximation will be evaluated. In order to judge the accuracy of these approximations, the results will be compared to the numerical solution of the Enskog equation by means of the direct simulation Monte Carlo (DSMC) method formulated by Bird[27] for the Boltzmann equation and extended to the Enskog equation by Montanero and Santos.[28] The results given below were obtained from runs in three dimensions using 10^5 points in a cubic volume of σ^3 with periodic boundaries. The time step used was 0.0117 mean free times and the length of the run was 2000 mean free times.

C. The local equilibrium approximation

The simplest approximation is to take $k_0 = 1$ which thus ignores all nonequilibrium corrections to the distribution. Then, as discussed in Appendix A, one has that

$$I^*_{1,00} = 2p(D+2)\Delta^* e^{-\Delta^*}, \tag{18}$$

and Eq. (7) becomes

$$\frac{d}{dt^*}\Delta^* = \Delta^{*3/2} e^{-\Delta^*}. \tag{19}$$

Thus, at this level of approximation, all details of the probability of an inelastic collision, the density and the dimensionality, can be scaled out of the expression for the temperature so that the temperature follows a universal curve. As expected, Eq. (19) gives a nonzero cooling rate for all values of the temperature. Note that the right hand side goes to zero in the two limits $\Delta^* \to 0$ and $\Delta^* \to \infty$. This reflects the fact that at very low temperatures, $\Delta^* \to \infty$, very few collisions occur with enough energy to be inelastic while at very high temperature, $\Delta^* \to 0$, the loss of energy during inelastic collisions is of no physical importance since it represents a vanishing fraction of the total energy of each atom. Both of these limits can therefore be viewed, in some sense, as "elastic" limits although in neither case can one say that only elastic collisions occur and it is to be expected that in both of these elastic limits, all thermodynamic and transport properties will be those of an elastic gas since the energy dissipation plays no role. The source term in Eq. (19) also exhibits a maximum at $\Delta^* = 3/2$ which is not surprising and, in fact, must be true of the exact cooling rate: since Δ^* goes to zero in the elastic limits it must either be constant or it must have at least one extremum. Nevertheless, when written in terms of dimensional quantities, the cooling equation becomes
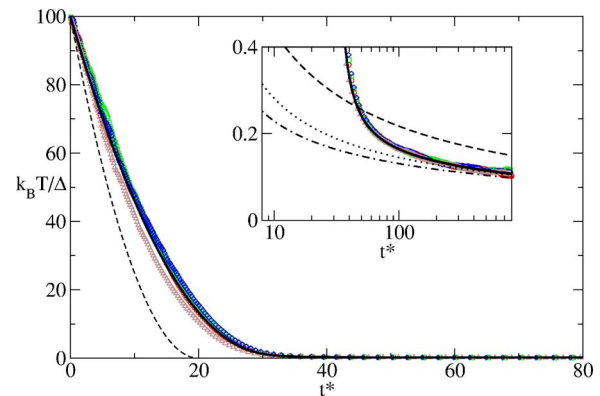
FIG. 1. The temperature as a function of time as predicted by Eq. (19) (line) and as determined from four different DSMC simulations (circles, squares, diamonds, and triangles). The theory and simulation results are indistinguishable. Note the very rapid, algebraic, decrease in the temperature at early times when the dimensionless temperature is large and the very slow, logarithmic, decay at long times when the dimensionless temperature is less than one. The dashed line in the main figure is the approximation given in Eq. (21). The dashed, dotted, and dashed-dotted lines in the inset correspond to keeping the first term, first two terms, and all three terms in the asymptotic approximation of Eq. (22).

$$\frac{d}{dt}T = -2p(D$$
$$+2)n^*\chi\frac{S_D}{2D(D+2)\sqrt{\pi}}\left(\frac{\Delta}{m\sigma^2}\right)^{1/2}\sqrt{\Delta k_B T}\,e^{-\Delta/k_B T}, \tag{20}$$

showing that the physical cooling rate is a monotonically increasing function of the temperature. For high temperatures, $\Delta^* = \beta\Delta \ll 1$ and has the approximate behavior

$$\Delta^*(t^*) \simeq \frac{\Delta^*(0)}{\left(1 - \frac{1}{2}\sqrt{\Delta^*(0)}\,t^*\right)^2}, \tag{21}$$

so that the temperature decays algebraically. When the temperature is low, $\Delta^* = \beta\Delta \gg 1$ and it can be shown (see Appendix B) that the cooling becomes very slow

$$\Delta^* = \ln t^* + \frac{3}{2}\ln(\ln t^*) + \frac{9}{4}\frac{\ln(\ln t^*)}{\ln t^*} + \cdots. \tag{22}$$

The full behavior is shown in Fig. 1 where the crossover between these two asymptotic forms is evident. As the figure shows, the theory is in good agreement with the simulations. In this approximation, the pressure is given by

$$\frac{p}{nk_B T} = 1 + n^*\chi\frac{S_D}{2D} + n^*\chi\frac{S_D}{4D}p\left(\left(1 - 2\sqrt{\frac{\Delta^*}{\pi}}\right)e^{-\Delta^*}\right.$$
$$\left. + (\mathrm{erf}(\sqrt{\Delta^*}) - 1)\right). \tag{23}$$

The first two terms on the right are the usual equilibrium expression and the third term represents the nonequilibrium correction. The effect of the nonequilibrium term is shown in Fig. 2 where it is seen that a minimum occurs in p/nkT near $\Delta/k_B T = 1$. The effect is small, the minimum being about 8%
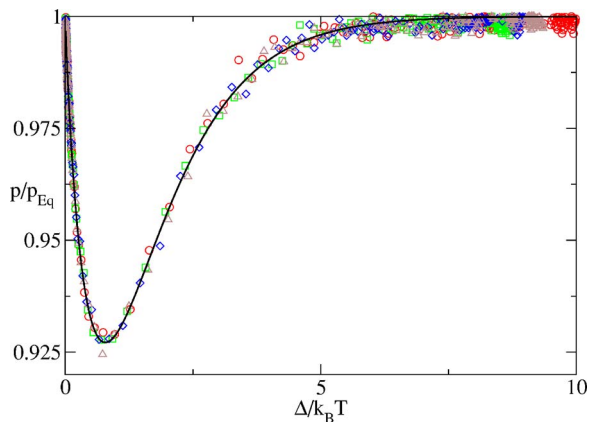
FIG. 2. The ratio of the pressure of the dissipative gas to that of an equilibrium $\Delta = 0$ gas as a function of Δ^* for a dense ($n^* = 0.5$) gas in three dimensions with $p = 1$. Different symbols correspond to results from separate simulations.

below the equilibrium value. Again, the theory and simulation are seen to be in good agreement.

D. First non-Gaussian correction

The simplest non-Gaussian correction consists of taking $k_0 = 2$. The required coefficients are, in addition to $I^*_{1,00}$ given above,

$$I^*_{2,00} = -2p\Delta^* e^{-\Delta^*}(\Delta^* - 1),$$

$$I^*_{1,02} + I^*_{1,20} = p\frac{D+2}{8}\Delta^* e^{-\Delta^*}(4\Delta^{*2} - 4\Delta^* - 1),$$

$$\tag{24}$$

$$I^*_{2,02} + I^*_{2,20} = -8(D-1) - \frac{1}{8}pe^{-\Delta^*}(4\Delta^{*4} - 8\Delta^{*3}$$

$$+ (75 + 16D)\Delta^{*2} + (69 - 24D)\Delta^*$$

$$+ 32(1-D)) - 2p(D-1)\Delta^* e^{-(1/2)\Delta^*} K_1\left(\frac{1}{2}\Delta^*\right),$$

where $K_\nu(x)$ is the modified Bessel function of the second kind. Equations (16) and (17) can be solved simultaneously
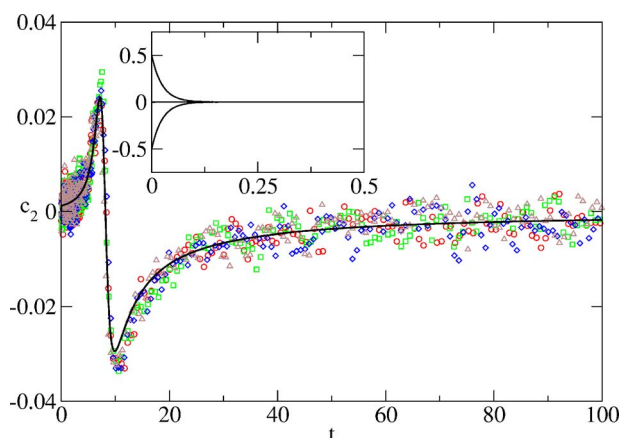
FIG. 3. The coefficient of the first non-Gaussian correction, c_2, as predicted by Eq. (17) (line) and as determined from four different DSMC simulations (different symbols). The inset shows the rapid convergence of the numerical solution for three different initial conditions.

given an initial temperature $\Delta^*(0)$ and a value for $c_2(t=0) = c_2(\Delta^* = \Delta^*(0))$. Figure 3 shows $c_2(t^*)$ for $n^* = 0.5$ in three dimensions as well as the results obtained from the simulation. The behavior of c_2 is seen to be highly nontrivial with a sharp change of sign at $\Delta^* = 1$ and, for longer times, a decay to zero. The inset shows that the initial condition for c_2 is irrelevant except at very short times. Overall, the agreement between the calculation and the simulation is very good. The small magnitude of c_2 indicates that the distribution can be well approximated by a Gaussian and the agreement of the pressure to the simulations support the view that the homogeneous state is well described by a local-equilibrium distribution.

III. TRANSPORT COEFFICIENTS

The Navier-Stokes equations for a dissipative system take the form[23]

$$\frac{\partial}{\partial t}n + \boldsymbol{\nabla} \cdot (\mathbf{u}n) = 0,$$

$$\frac{\partial}{\partial t}\mathbf{u} + \mathbf{u} \cdot \boldsymbol{\nabla}\mathbf{u} + \frac{1}{\rho}\boldsymbol{\nabla} \cdot P = 0,$$

$$\tag{25}$$

$$\left(\frac{\partial}{\partial t} + \mathbf{u} \cdot \boldsymbol{\nabla}\right)T + \frac{2}{Dnk_B}[\overset{\leftrightarrow}{P} : \boldsymbol{\nabla}\mathbf{u} + \boldsymbol{\nabla} \cdot \mathbf{q}] = \xi_0 + \xi_1\boldsymbol{\nabla} \cdot \mathbf{u},$$

with pressure tensor

$$P_{ij} = p^{(0)}\delta_{ij} - \eta\left(\partial_i u_j + \partial_j u_i - \frac{2}{D}\delta_{ij}(\boldsymbol{\nabla} \cdot \mathbf{u})\right) - \gamma\delta_{ij}(\boldsymbol{\nabla} \cdot \mathbf{u})$$

$$\tag{26}$$

and heat-flux vector

$$\mathbf{q}(\mathbf{r},t) = -\mu\boldsymbol{\nabla}\rho - \kappa\boldsymbol{\nabla}T. \tag{27}$$

There are two differences between these equations and the Navier-Stokes equations for an elastic fluid. First, the temperature equation contains source terms that account for the collisional cooling. Second, the heat-flux vector depends on gradients in density as well as temperature. Both of these contributions are well known from the study of granular media. In this section, the expressions for the various transport coefficients and source terms are discussed for the dissipative interaction model.

For equilibrium fluids, the transport coefficients are algebraic functions of the temperature and density. This is no longer true in the present case and the transport coefficients must be determined by solving ordinary differential equations as was also the case with c_2 above. In the following, we evaluate the expressions for the transport coefficients given in Ref. 25 in the approximation that $c_2 = 0$. Then, from the previous section, one has that

$$\xi_0 = -\frac{Dnk_BT}{2}n^*\chi\frac{S_D}{2D(D+2)\sqrt{\pi}}\left(\frac{k_BT}{m\sigma^2}\right)^{1/2}I^*_{1,00}. \tag{28}$$

It is convenient to express the transport coefficients in terms of dimensionless functions by writing
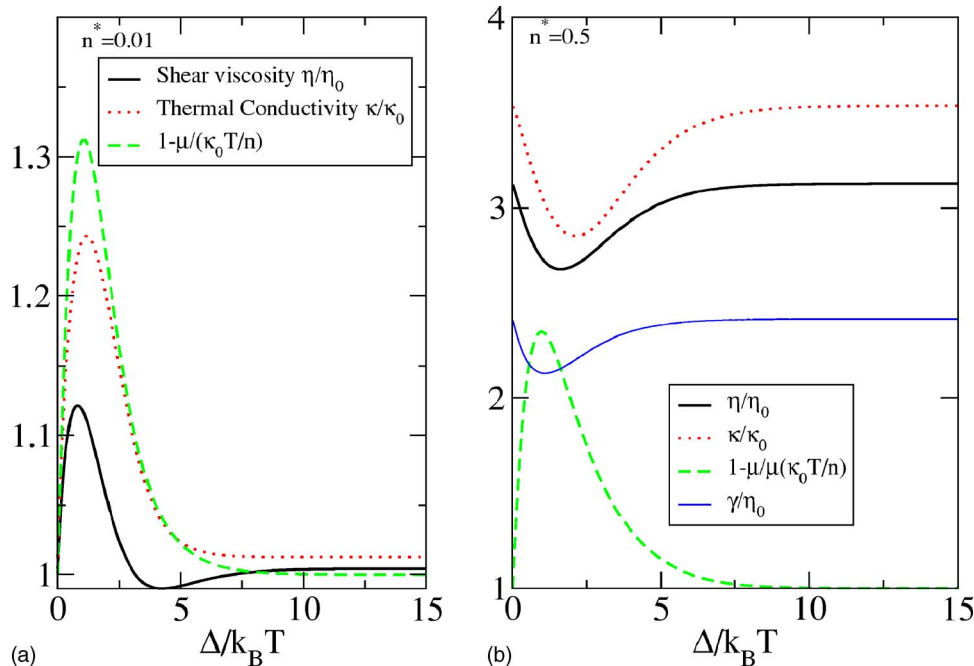
FIG. 4. The dimensionless transport coefficients as functions of the reduced temperature for a three-dimensional gas with $p=1$ and for (a) a low-density, $n^*=0.01$, gas and (b) a high-density, $n^*=0.5$, gas.

$$\eta = \eta_0 \bar{\eta},$$

$$\gamma = \eta_0 \bar{\gamma},$$

$$\mu = \kappa_0 \frac{T}{n} \bar{\mu},$$

$$\kappa = \kappa_0 \bar{\kappa},$$

(29)

where the Boltzmann transport coefficients for an elastic gas are

$$\eta_0 = \sqrt{m k_B T} \frac{(D+2)\sqrt{\pi}}{4 S_D} \sigma^{1-D},$$

$$\kappa_0 = k_B \sqrt{\frac{k_B T}{m}} \frac{D(D+2)^2 \sqrt{\pi}}{8 S_D (D-1)} \sigma^{1-D}.$$

(30)

Then, the transport coefficients can be written in terms of their kinematic contributions as

$$\bar{\eta} = \left(1 + \frac{2}{3}\bar{\theta}\right)\bar{\eta}^K + \frac{D}{D+2}\bar{\gamma}_1,$$

$$\bar{\gamma} = \bar{\gamma}^K + \bar{\gamma}_1,$$

$$\bar{\mu} = (1 + \bar{\theta})\bar{\mu}^K,$$

(31)

$$\bar{\kappa} = (1 + \bar{\theta})\bar{\kappa}^K + \frac{D-1}{D+2}\bar{\gamma}_1,$$

where the auxiliary functions $\bar{\gamma}_1(n^*, \Delta^*)$ and $\bar{\theta}(n^*, \Delta^*)$ are given in Appendix C.

As shown in Appendix C, the kinematic contributions to the transport coefficients satisfy the equations

$$I_{1,00}^* \Delta^* \frac{\partial \bar{\eta}^K}{\partial \Delta^*} + \left(8 D I_\eta^* - \frac{1}{2}I_{1,00}^*\right)\bar{\eta}^K = \frac{8D}{\chi} + 8 n^* \frac{S_D}{D+2}\Omega_\eta^*,$$

$$I_{1,00}^* \Delta^* \frac{\partial}{\partial \Delta^*}\bar{\gamma}^K + \left(8(D-1)I_\lambda^* - \frac{3}{2}I_{1,00}^*\right)\bar{\gamma}^K = 16\sqrt{\pi}\Omega_\gamma^*,$$

$$I_{1,00}^* \Delta^* \frac{\partial \bar{\kappa}^K}{\partial \Delta^*} + (8(D-1)I_\kappa^* - (1+\Delta^*)I_{1,00}^*)\bar{\kappa}^K$$

(32)

$$= 8\frac{D-1}{\chi} + \frac{12(D-1)}{D(D+2)}n^* S_D \Omega_\kappa^*,$$

$$I_{1,00}^* \Delta^* \frac{\partial \bar{\mu}^K}{\partial \Delta^*} + \left(8(D-1)I_\mu^* - \frac{3}{2}I_{1,00}^*\right)\bar{\mu}^K$$

$$+ I_{1,00}^*\left(1 + n\frac{\partial \ln \chi_0}{\partial n}\right)\bar{\kappa}^K = \Omega_\mu^*,$$

where explicit expressions for the Boltzmann integrals, I_α^*, and the sources, Ω_α^*, are given in Appendix C. For both an elastic hard-sphere gas as well as a simple granular fluid, the dimensionless transport coefficients are only functions of the density so that the derivative terms vanish and these reduce to a system of simple algebraic equations. Here, the presence of an additional energy scale leads to a more complex dependence on temperature.

Figure 4 shows the transport coefficients for a low density, $n^*=0.01$, and a moderately dense density gas, $n^*=0.5$, with $p=1$ in three dimensions as a function of temperature as obtained by solving these equations with the initial condition that the scaled transport coefficients take on their equilibrium values at $\Delta^*=0$. The behavior of the transport coefficients is
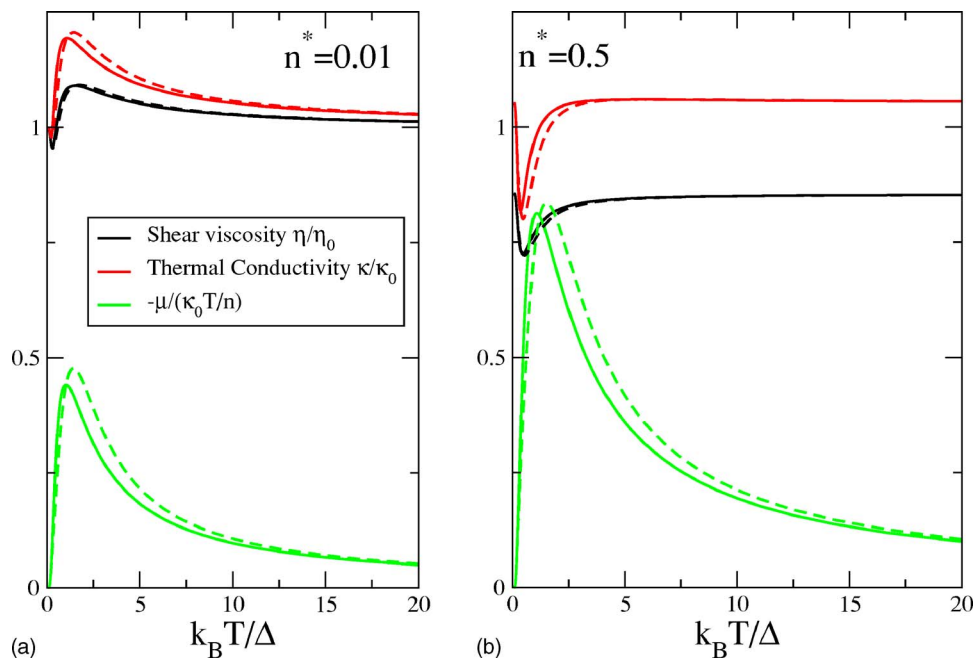
FIG. 5. The dimensionless kinetic contributions to the transport coefficients as functions of the reduced temperature. The broken lines are from the adiabatic approximation. The upper lines are the thermal conductivity, the middle lines are the shear viscosity, and the bottom lines are $-\mu$.

nonmonotonic with a "resonance" occurring in the vicinity of $\Delta^* = 1$. For the thermal conductivity and the shear viscosity, the effect is a reduction of about 20% compared to the equilibrium transport coefficients while the effect on the bulk viscosity is minimal. The new transport coefficient μ is surprisingly large, being of order 1 up to $3 \gtrsim \Delta^* \gtrsim 0.05$ and is of order 0.1 for $5 \gtrsim \Delta^* \gtrsim 0.01$.

Since in both the elastic and the simple granular fluids,[25] the scaled transport coefficients do not depend on temperature, a simpler and more practical approximation suggests itself is to drop the derivatives in Eqs. (32) giving

$$\left(8DI_\eta^* - \frac{1}{2}I_{1,00}^*\right)\bar\eta^K = \frac{8D}{\chi} + 8n^*\frac{S_D}{D+2}\Omega_\eta^*,$$

$$\left(8(D-1)I_\lambda^* - \frac{3}{2}I_{1,00}^*\right)\bar\gamma^K = 16\sqrt{\pi}\Omega_\gamma^*,$$

$$(8(D-1)I_\kappa^* - (1+\Delta^*)I_{1,00}^*)\bar\kappa^K = 8\frac{D-1}{\chi} + \frac{12(D-1)}{D(D+2)}n^*S_D\Omega_\kappa^*,$$

(33)

$$\left(8(D-1)I_\mu^* - \frac{3}{2}I_{1,00}^*\right)\bar\mu^K + I_{1,00}^*\left(1 + n\frac{\partial \ln\chi_0}{\partial n}\right)\bar\kappa^K = \Omega_\mu^*,$$

which will be termed the adiabatic approximation. Figure 5 shows that Eq. (33) provides a reasonable approximation to the full results obtained by integrating Eqs. (32). The reason for the resonance in the transport coefficients is now easier to see: the Boltzmann integrals $I_\eta^*, \dots$ are scaled so as to go to one in the elastic limits $\Delta^* \to 0$ and $\Delta^* \to \infty$ when the energy loss is negligible and necessarily exhibits at least one extremum in between. The interaction of these functions with the

cooling term $I_{1,00}^*$, which behaves similarly with a maximum at $\Delta^* = 1$, gives rise to the resonances in the transport coefficients reflecting the fact that the effect of the dissipation is at its maximum somewhere in between those limits.

IV. APPLICATION: THE CIRCULAR PISTON

In this section, to illustrate the importance of the coupling of energy loss and hydrodynamics, the behavior of a gas confined to a contracting circular piston, described in Ref. 20, is reexamined for the case of the model gas considered here. To this end, the modified Navier-Stokes equations, Eqs. (25)–(27), have been solved numerically with a hard circular boundary moving at constant speed c under the assumption of circular symmetry. The gas is initially in a uniform state at temperature $T(0)$ and here the focus will be on the particular case examined in Ref. 20 that the wall moves with speed $c = -5\sqrt{k_B T(0)/m}$ and initial number density $n^*(0) = 0.1$. The energy gap parameter will be reported scaled to the initial temperature as $\Delta^* = \Delta/k_B T(0)$. Time will be reported in units $\tau = \sqrt{m\sigma^2/2k_B T(0)}$ and all calculations are performed with $p = 1$ and using the pressure given in Eq. (23) and the transport coefficients evaluated using the adiabatic approximation introduced above.

Figure 6(a) shows a comparison of the resulting shock waves for the two cases: $\Delta^* = 0$, an elastic gas, and $\Delta^* = 20$, a highly inelastic gas, after the same elapsed time. It is clear that the inelasticity leads to a substantial slowing of the shock waves as well as a dramatic change in the shape of the temperature profile. Shown in Fig. 6(b) is a comparison of the same profiles for the elastic case to the profiles for the inelastic gas at a later time when the shock waves are at approximately the same position. From this comparison, it is clear that the pressure and velocity profiles are, in fact, quite similar for the two cases and that most difference lies in the temperature profile where that of the inelastic gas appears more like a localized pulse than a shock. A similar compari-
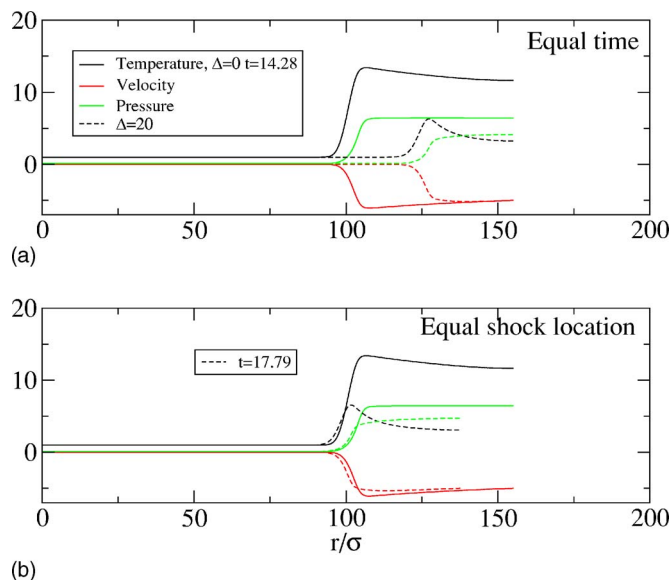
FIG. 6. Snapshots of the temperature, pressure, and velocity profiles as functions of distance from the center of the circle, r, for the elastic (full lines) and inelastic (broken lines) gases. The upper lines are the temperature, the middle lines the pressure and the lower lines the velocities. (a) shows profiles at equal times, $t=14.28\tau$, while in (b) the inelastic profile was taken at $t=17.79\tau$ so as to show the shocks at approximately equal positions.

son is made in Fig. 7 for a time just before the shocks are focused at the center of the bubble. The same qualitative features appear: the shock in the inelastic gas is significantly retarded compared to the elastic gas and all profiles are similar, when compared at equal shock position, except for the temperature profile. The fact that the pressure profiles are similar even though the temperature profiles are dramatically different is due to a compensation in the density profiles, as shown in Fig. 8. Since the shocks in the inelastic gas travel much more slowly than those in the elastic gas, the density in the high-density region is necessarily higher in the inelastic case since mass must be conserved. At the high densities that
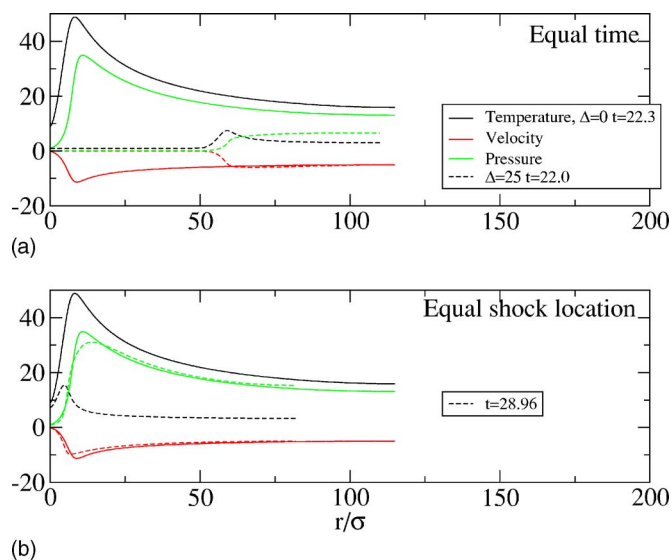
FIG. 7. The same as Fig. 6 except for times when the shocks have nearly reached the center of the bubbles. The times shown are $t=22.3\tau$ in (a) and for the elastic profile in (b) and $t=28.96\tau$ for the inelastic profile in (b).
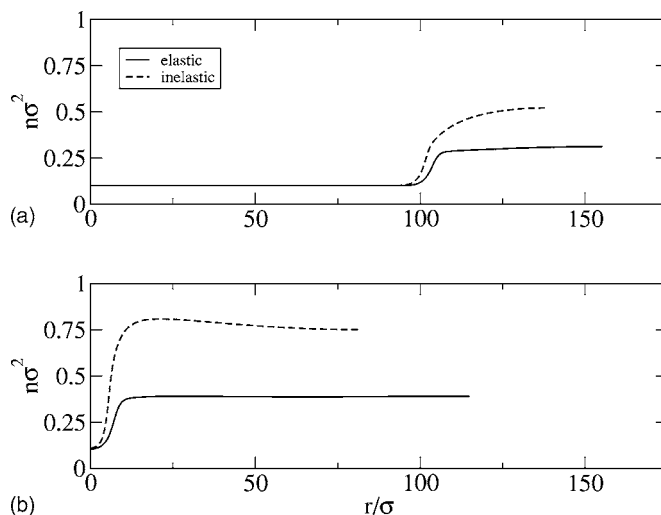
FIG. 8. Density profiles for the early (a) and later (b) times of Figs. 6(b) and 7(b), respectively. The full lines are for the elastic gas and the broken lines for the inelastic gas.

occur as the shocks are focused, the excluded volume effects become significant and lead to large contributions to the pressure. In fact, the densities are so high, close to random close packing, that the model used for the pair distribution function at contact, $\chi(n)$, is inaccurate and the pressure effects are undoubtedly underestimated.

The maximum temperature achieved in the center of the bubble, T_{max}, is shown in Fig. 9 as a function of Δ^*. Recall that since Δ is both the energy threshold for inelastic collisions and the amount of energy lost during an inelastic collision, there are two elastic limits: $\Delta \rightarrow \infty$, corresponding to an infinite threshold so that no inelastic collisions occur, and $\Delta \rightarrow 0$, corresponding to the degenerate case of all collisions being "inelastic" but the energy loss being zero. Starting from the first elastic limit, $\lim_{\Delta^* \rightarrow \infty} T_{max}=198T(0)$, the maximum temperature decreases as Δ^* decreases as would be expected since lower values mean that more atoms can participate in inelastic collisions. A minimum is reached near
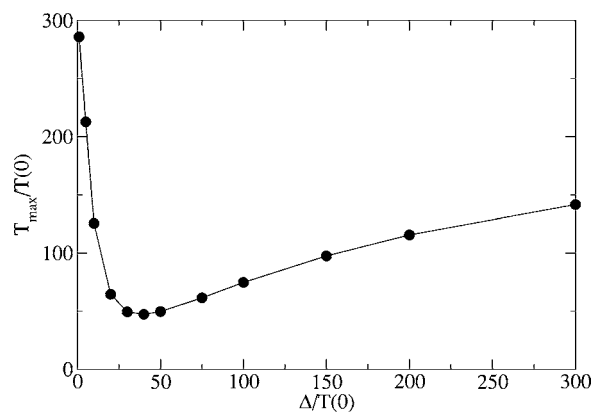
FIG. 9. Maximum temperature as a function of Δ.

$\Delta^*=40$ where $T_{max}\sim 47T(0)$. It is interesting that at this minimum in $T_{max}(\Delta^*)$, one has $\Delta/T_{max}\sim 1$ so that the cooling that occurs is maximal according to Eq. (19). For smaller values of Δ^*, the maximum temperature increases which is not surprising since the elastic limit is again recovered at $\Delta=0$. What is surprising, however, is that at $\Delta^*=1$ the maximum temperature is $284T(0)$ or about 50% *higher* than in the elastic, $\Delta^*=0$, case. The explanation of this result is that for the range of Δ under consideration the speed of the shocks, and the increase in the density behind them, increases monotonically as Δ decreases thus leading to higher pressures, and higher rates of viscous heating, at the moment the shocks are focused. This interpretation is supported by the fact that eliminating the divergence of the pressure at high densities by setting $\chi(n)\rightarrow\chi(n(0))$ in the evaluation of the pressure eliminates the increase in maximal temperature as Δ^* decreases to one. That only leaves the question as to why the shock slows down. To answer that, the calculations were repeated with all transport properties and the pressures are evaluated using the expressions for an elastic gas so that the only effect of the inelasticity is through the cooling rate. The result is that the shocks are still slow and that the qualitative behavior of the maximal temperature is unchanged leading to the conclusion that the slowing of the shock is solely due to the ξ_0 term in the heat equation.

As Δ^* decreases from one, the maximum temperature begins to decrease. However, the numerical code used becomes unstable in the range $0.8>\Delta^*>0.2$ so it is not possible to follow this behavior further. The instability may be due to deficiencies in the code but a more intriguing possibility is that this indicates a real hydrodynamic instability due to a pressure inversion as occurs in granular fluids. A pressure inversion occurs when the compressibility becomes negative due to the fact that an increase in density leads to such a decrease in temperature that the pressure decreases with increasing density.

V. CONCLUSIONS

In this paper, a simple model of a gas exhibiting couplings between hydrodynamics and chemistry, in the form of inelastic collisions, has been explored. The model consists of hard spheres that lose a fixed amount of energy, Δ, if the collisional energy is sufficient. This model was inspired by the simplest prototype for an activated chemical reaction wherein the reaction can only take place if there is sufficient kinetic energy during collisions.[29] It was found that in contrast to the well-known behavior of granular systems, the fixed energy loss model studied here gives rise to a homogeneous cooling state that is well described by a Gaussian distribution. The cooling is algebraic in time for temperatures much larger than the energy loss, Δ, and logarithmic for temperatures much smaller than Δ. While the cooling rate grows monotonically with temperature, it was found that the rate of change of the physically relevant variable $\Delta^*=\Delta/k_BT$ has a maximum at the value $\Delta^*=1.5$ and that this gives rise to numerous nonmonotonic temperature

dependencies in the thermodynamic and transport properties of the system. In particular, in the homogeneous state, the coefficients of the first non-Gaussian corrections to the distribution involve rapid changes near this value and yet are well predicted by kinetic theory as demonstrated by comparison to numerical solutions of the Enskog equation. Explicit expressions for the transport coefficients were given and it was shown that a relatively simple and accurate "adiabatic" approximation existed. The transport coefficients show "resonances" which are again related to the nonmonotonicity of the rate of change of Δ^*.

As an application, the hydrodynamic description thus specified was used to study the behavior of shocks in a two-dimensional circular piston. It was found that the maximum temperature obtained when the shocks were focused at the center of the volume exhibits a minimum as a function of $\Delta/k_BT(0)$ at about $\Delta/k_BT(0)=40$ and rises to a maximum near $\Delta/k_BT(0)=1$. Below this value it appears that the fluid becomes unstable, perhaps due to a pressure inversion. It is interesting to note that for a gas at room temperature, $k_BT(0)\sim 300$ K so the minimum occurs at $\Delta\sim 12\,000$ K or, roughly, 1 eV which is clearly a physically relevant value for sonochemistry. The picture here is therefore more complex than that found in the study of the effect of energy loss on the maximum temperature using adiabatic models (i.e., assuming uniform density and temperature in the gas).[10,16] On hand, the present results show that for a large range of values, $\Delta>12\,000$ K, the dissipation leads to a substantial reduction of the maximum temperature—at the minimum, the maximum temperature is only 20% of that predicted for an elastic system—in agreement with the predictions of Yasui.[10] On the other hand, for the physically important range 300 K $<\Delta<12\,000$ K, the maximal temperature increases rapidly with decreasing Δ, eventually reaching values 50% greater than those predicted in an elastic system. This increase is attributed entirely to excluded volume effects, in agreement with the results of Toegel *et al.*,[16] driven by the effect of the cooling in slowing down the shocks and leading to much increased densities behind the shock front.

The present study is only a first step in understanding the coupling of chemistry and hydrodynamics that is undoubtedly important in sonochemistry. Several open questions remain. First, it would be useful to be able to relate the cooling to the shock velocity. In particular, one could imagine doing this at the level of the Euler equations, which are analytically tractable in the case of an elastic fluid.[20] Second, it would be interesting to consider richer models with multiple species and real endothermic chemical interactions. Finally, and perhaps most interesting, would be to simply extend these results to three dimensions and with a coupling to the Rayleigh-Plesset equation.

APPENDIX A: DETAILS OF THE HCS CALCULATIONS

In Ref. 25, it was shown that the coefficients $I_{rs,k}$ which determine the HCS could be calculated as

$$I_{rs,k} = -n^* \frac{\Gamma\left(\frac{1}{2}D\right)\Gamma(k+1)}{\Gamma\left(\frac{1}{2}D+k\right)} \left(\frac{2k_BT}{m\sigma^2}\right)^{1/2} \frac{1}{r!s!k!} \lim_{z_1 \to 0} \lim_{z_2 \to 0} \lim_{x \to 0} \frac{\partial^r}{\partial z_1^r}\frac{\partial^s}{\partial z_2^s}\frac{\partial^k}{\partial x^k}\left[\sum_a G_a(\Delta_a) - G_0\right] \tag{A1}$$

with

$$G_a(\psi_t|\Delta_a) = -\frac{1}{2}\pi^{-1/2}S_D(1-z_1x)^{-(1/2)D}\left(\frac{1-z_1x}{2-x-z_2-z_1+xz_1z_2}\right)^{1/2}\int_0^\infty du K_a^*(\sqrt{u})\exp\left(\frac{(2-z_2-z_1)x}{2-x-z_2-z_1+xz_1z_2}\frac{1}{2}\Delta_a^*(\sqrt{u})\right)$$

$$\times \exp\left(-\frac{1-z_2x}{2-x-z_2-z_1+xz_1z_2}u\right)\exp\left(-\frac{1}{2}\frac{(z_2-z_1)x}{2-x-z_2-z_1+xz_1z_2}(u-\sqrt{u}\sqrt{u-2\Delta_a^*(\sqrt{u})})\right) \tag{A2}$$

and

$$G_0 = -\frac{1}{2}\pi^{-1/2}S_D(1-z_1x)^{-(D+1)/2}(2-x-z_2-z_1+xz_1z_2)^{1/2}. \tag{A3}$$

In the present case,

$$K_0^*(\sqrt{u}) = K_0\left(\sqrt{\frac{2u}{m\beta}}\right) = 1 - p\Theta\left(\frac{u}{2\beta}-\Delta\right) = 1 - p\Theta(u-2\beta\Delta),$$

$$\tag{A4}$$

$$K_1^*(\sqrt{u}) = K_1\left(\sqrt{\frac{2u}{m\beta}}\right) = p\Theta\left(\frac{u}{2\beta}-\Delta\right) = p\Theta(u-2\beta\Delta),$$

and $\Delta_0^*(\sqrt{u})=0$ and $\Delta_1^*(\sqrt{u})=\beta\Delta$. For this model, the coefficients can be more conveniently written as

$$I_{rs,k} = I_{rs,k}^E + I_{rs,k}^I \tag{A5}$$

with an elastic part defined by

$$I_{rs,k}^E = -n^* \frac{\Gamma\left(\frac{1}{2}D\right)\Gamma(k+1)}{\Gamma\left(\frac{1}{2}D+k\right)} \left(\frac{2k_BT}{m\sigma^2}\right)^{1/2} \frac{1}{r!s!k!} \lim_{z_1 \to 0} \lim_{z_2 \to 0} \lim_{x \to 0} \frac{\partial^r}{\partial z_1^r}\frac{\partial^s}{\partial z_2^s}\frac{\partial^k}{\partial x^k}[G_E - G_0], \tag{A6}$$

where the elastic generating function is

$$G_E = -\frac{1}{2}\pi^{-1/2}S_D(1-z_1x)^{-(1/2)D}\left(\frac{1-z_1x}{2-x-z_2-z_1+xz_1z_2}\right)^{1/2} \times \int_0^\infty du \exp\left(-\frac{1-z_2x}{2-x-z_2-z_1+xz_1z_2}u\right)$$

$$= -\frac{1}{2}\pi^{-1/2}S_D(1-z_1x)^{-(1/2)D}\left(\frac{2-x-z_2-z_1+xz_1z_2}{1-z_2x}\right)^{1/2} \tag{A7}$$

and an inelastic contribution

$$I_{rs,k}^I = -pn^* \frac{\Gamma\left(\frac{1}{2}D\right)\Gamma(k+1)}{\Gamma\left(\frac{1}{2}D+k\right)} \left(\frac{2k_BT}{m\sigma^2}\right)^{1/2} \frac{1}{r!s!k!} \lim_{z_1 \to 0} \lim_{z_2 \to 0} \lim_{x \to 0} \frac{\partial^r}{\partial z_1^r}\frac{\partial^s}{\partial z_2^s}\frac{\partial^k}{\partial x^k}G(\Delta^*) \tag{A8}$$

with the inelastic generating function

$$G(\Delta) = -\frac{1}{2}\pi^{-1/2}S_D(1-z_1x)^{-(1/2)D}\left(\frac{1-z_1x}{2-x-z_2-z_1+xz_1z_2}\right)^{1/2} \times \int_{2\Delta}^\infty du \exp\left(-\frac{1}{2}\frac{2-xz_1-xz_2}{2-x-z_2-z_1+xz_1z_2}u\right)$$

$$\times \left[\exp\left(\frac{1}{2}\frac{(2-z_2-z_1)x\Delta+(z_2-z_1)x\sqrt{u}\sqrt{u-2\Delta}}{2-x-z_2-z_1+xz_1z_2}\right) - \exp\left(\frac{1}{2}\frac{(z_2-z_1)xu}{2-x-z_2-z_1+xz_1z_2}\right)\right]. \tag{A9}$$

A change of variables in the integral gives

$$G(\Delta) = -\frac{1}{2}\pi^{-1/2}S_D(1-z_1x)^{-(1/2)D}\left(\frac{1-z_1x}{2-x-z_2-z_1+xz_1z_2}\right)^{1/2}\exp\left(-\frac{1}{2}\frac{2-xz_1-xz_2}{2-x-z_2-z_1+xz_1z_2}\Delta\right)$$

$$\times\Delta\int_1^{\infty}\exp\left(-\frac{1}{2}\frac{2-xz_1-xz_2}{2-x-z_2-z_1+xz_1z_2}\Delta y\right)\left[\exp\left(\frac{1}{2}\frac{(2-z_2-z_1)x\Delta+(z_2-z_1)x\Delta\sqrt{y^2-1}}{2-x-z_2-z_1+xz_1z_2}\right)\right.$$

$$\left.-\exp\left(\frac{1}{2}\frac{(z_2-z_1)x\Delta(y+1)}{2-x-z_2-z_1+xz_1z_2}\right)\right]dy. \tag{A10}$$

Using

$$\int_1^{\infty}\exp\left(-\frac{1}{2}\frac{2-xz_1-xz_2}{2-x-z_2-z_1+xz_1z_2}\Delta y+\frac{1}{2}\frac{(z_2-z_1)x\Delta\sqrt{y^2-1}}{2-x-z_2-z_1+xz_1z_2}\right)dy$$

$$=\sum_{n=0}^{\infty}\frac{1}{n!}\left(\frac{1}{2}\frac{(z_2-z_1)x\Delta}{2-x-z_2-z_1+xz_1z_2}\right)^n\int_1^{\infty}\exp\left(-\frac{1}{2}\frac{2-xz_1-xz_2}{2-x-z_2-z_1+xz_1z_2}\Delta y\right)(y^2-1)^{n/2}dy$$

$$=\frac{2}{\sqrt{\pi}}\sum_{n=0}^{\infty}\frac{\Gamma\left(\frac{1}{2}n+1\right)}{\Gamma(n+1)}\Delta^{(n-1)/2}F_n(x,z_1,z_2;\Delta) \tag{A11}$$

with

$$F_n(x,z_1,z_2;\Delta)=(z_2-z_1)^nx^n(2-x-z_2-z_1+xz_1z_2)^{-(n-1)/2}(2-xz_1-xz_2)^{-(n+1)/2}K_{(n+1)/2}\left(\frac{1}{2}\frac{2-xz_1-xz_2}{2-x-z_2-z_1+xz_1z_2}\Delta\right) \tag{A12}$$

and

$$\int_1^{\infty}\exp\left(-\frac{1}{2}\frac{2-xz_1-xz_2}{2-x-z_2-z_1+xz_1z_2}\Delta y\right)\exp\left(\frac{1}{2}\frac{(z_2-z_1)x\Delta(y+1)}{2-x-z_2-z_1+xz_1z_2}\right)dy$$

$$=\exp\left(\frac{1}{2}\frac{(z_2-z_1)x\Delta}{2-x-z_2-z_1+xz_1z_2}\right)\int_1^{\infty}\exp\left(-\frac{1-z_2x}{2-x-z_2-z_1+xz_1z_2}\Delta y\right)dy$$

$$=\exp\left(-\frac{1}{2}\frac{2-3xz_2+xz_1}{2-x-z_2-z_1+xz_1z_2}\Delta\right)\left(\frac{1-z_2x}{2-x-z_2-z_1+xz_1z_2}\Delta\right)^{-1} \tag{A13}$$

gives

$$G(\Delta)=-\frac{1}{2}\pi^{-1/2}S_D(1-z_1x)^{-(1/2)D}\left(\frac{1-z_1x}{2-x-z_2-z_1+xz_1z_2}\right)^{1/2}\times\exp\left(-\frac{1-x}{2-x-z_2-z_1+xz_1z_2}\Delta\right)$$

$$\times\left[\frac{2}{\sqrt{\pi}}\sum_{n=0}^{\infty}\frac{\Gamma\left(\frac{1}{2}n+1\right)}{\Gamma(n+1)}\Delta^{(n+1)/2}F_n(x,z_1,z_2;\Delta)-\left(\frac{2-x-z_2-z_1+xz_1z_2}{1-z_2x}\right)\exp\left(-\frac{1}{2}\frac{2-4z_2x+2x}{2-x-z_2-z_1+xz_1z_2}\Delta\right)\right]. \tag{A14}$$

Notice that in order to evaluate $I_{rs,k}$, only the first $r+s$ terms of the sum need be retained. Thus, for example, using $K_{1/2}(x)=\sqrt{(\pi/2x)}e^{-x}$ one has that

$$\lim_{z_1\to 0}\lim_{z_2\to 0}G(\Delta)=-\frac{1}{2}\pi^{-1/2}S_D(2-x)^{1/2}(e^{-\Delta}-e^{2\Delta/(x-2)}) \tag{A15}$$

and

$$I_{k,00} = I_{k,00}^I = -pn^*\chi \frac{\Gamma\left(\frac{1}{2}D\right)}{\Gamma\left(\frac{1}{2}D+k\right)} \left(\frac{2k_BT}{m\sigma^2}\right)^{1/2} \lim_{z_1\to 0}\lim_{z_2\to 0}\lim_{x\to 0} \frac{\partial^k}{\partial x^k}G(\Delta^*)$$

$$= \frac{S_D pn^*\chi}{2\sqrt{\pi}} \frac{\Gamma\left(\frac{1}{2}D\right)}{\Gamma\left(\frac{1}{2}D+k\right)} \left(\frac{2k_BT}{m\sigma^2}\right)^{1/2} \lim_{x\to 0} \frac{\partial^k}{\partial x^k}(2-x)^{1/2}(e^{-\Delta^*}-e^{2\Delta^*/(x-2)}), \tag{A16}$$

so that

$$I_{1,00} = \frac{S_D pn^*\chi}{D\sqrt{\pi}}\left(\frac{k_BT}{m\sigma^2}\right)^{1/2}\Delta^* e^{-\Delta^*}, \qquad I_{2,00} = \frac{S_D PN^*\chi}{D(D+2)\sqrt{\pi}}\left(\frac{K_BT}{M\sigma^2}\right)^{1/2}(1-\Delta^*)\Delta^* E^{-\Delta^*}. \tag{A17}$$

APPENDIX B: COOLING RATE

The cooling rate is well described by the equation

$$\frac{d}{dt^*}\Delta^* = \Delta^{*3/2}e^{-\Delta^*}. \tag{B1}$$

If the initial temperature is high, so that $\Delta^*(0) \ll 1$, then for short times

$$\frac{d}{dt^*}\Delta^* \simeq \Delta^{*3/2}, \tag{B2}$$

which is easily solved to give

$$\Delta^*(t^*) \simeq \frac{\Delta^*(0)}{\left(1-\frac{1}{2}\sqrt{\Delta^*(0)}t^*\right)^2}, \tag{B3}$$

suggesting that $\Delta^* \to \infty$ and $T \to 0$ at $t^* = \sqrt{4k_BT(0)/\Delta}$. This obviously does not happen and instead, the long-time behavior, corresponding to $\Delta^* \gg 1$, can be determined by writing Eq. (B1) as

$$t^* = \int_{\Delta^*(0)}^{\Delta^*} x^{-3/2}e^x dx$$

$$= 2\frac{e^{\Delta^*(0)}}{\sqrt{\Delta^*(0)}} + 2i\sqrt{\pi}\,\text{erf}(i\sqrt{\Delta^*(0)}) - 2\frac{e^{\Delta^*}}{\sqrt{\Delta^*}}$$

$$- 2i\sqrt{\pi}\,\text{erf}(i\sqrt{\Delta^*}). \tag{B4}$$

Now

$$\text{erf}(ix) = i\pi^{-1/2}e^{x^2}\left(\frac{1}{x} + \frac{1}{2x^3} + \frac{3}{4x^5} + \cdots\right) \tag{B5}$$

so, defining $\gamma = -2e^{\Delta^*(0)}/\sqrt{\Delta^*(0)} - 2i\sqrt{\pi}\,\text{erf}(i\sqrt{\Delta^*(0)})$,

$$t^* = -2\frac{e^{\Delta^*}}{\sqrt{\Delta^*}} + 2\frac{e^{\Delta^*}}{\sqrt{\Delta^*}}\left(1 + \frac{1}{2\Delta^*} + \frac{3}{4\Delta^{*2}} + \cdots\right) - \gamma$$

$$= \frac{e^{\Delta^*}}{\Delta^{*3/2}}\left[1 + \frac{3}{2\Delta^*} + \cdots - \gamma e^{-\Delta^*}\Delta^{*-3/2}\right]. \tag{B6}$$

Keeping only the leading order term and taking the log give

$$\ln t^* = \Delta^* - \frac{3}{2}\ln \Delta^*. \tag{B7}$$

At long times, Δ^* will be large so that the first term on the right dominates showing that $\Delta^* \sim \ln t^*$. Treating the last term on the right as being a perturbation, a series solution can be developed. The result is $\Delta^* = \Sigma_{k=0}\Delta_k^*$ with the first few terms given by

$$\begin{aligned}
\Delta_0^* &= \ln t^*, \\
\Delta_1^* &= \frac{3}{2}\ln \Delta_0^*, \\
\Delta_2^* &= \frac{3}{2}\frac{\Delta_1^*}{\Delta_0^*}, \\
\Delta_3^* &= \frac{3}{2}\frac{\Delta_2^*}{\Delta_0^*} - \frac{3}{4}\frac{\Delta_1^{*2}}{\Delta_0^{*2}}, \\
\Delta_4^* &= \frac{3}{2}\frac{\Delta_3^*}{\Delta_0^*} + \frac{1}{2}\frac{\Delta_1^*\Delta_2^*}{\Delta_0^{*2}} + \frac{1}{2}\frac{2\Delta_2^*\Delta_0^* - \Delta_1^{*2}}{\Delta_0^{*3}}\Delta_1^*.
\end{aligned} \tag{B8}$$

Numerical calculations confirm that only the first three terms give significant contributions.

APPENDIX C: THE TRANSPORT COEFFICIENTS

1. Total transport coefficients

With the approximation $c_2 = 0$, the transport coefficients can be written in terms of their kinetic contributions as

$$\begin{aligned}
\eta &= \left(1 + \frac{2}{3}\bar{\theta}\right)\eta^K + \frac{D}{D+2}\eta_0\bar{\gamma}_1, \\
\gamma &= \gamma^K + \eta_0\bar{\gamma}_1, \\
\mu &= (1+\bar{\theta})\mu^K, \\
\kappa &= (1+\bar{\theta})\kappa^K + \frac{D}{2}\frac{k_B}{m}\eta_0\bar{\gamma}_1,
\end{aligned} \tag{C1}$$

with the auxiliary functions

$$\gamma_1 = \eta_0 \frac{4S_D^2}{\pi(D+2)D^2} n^{*2} \chi \left[1 + \frac{1}{4} p \int_{\sqrt{2\Delta^*}}^{\infty} e^{-(1/2)v^2} v^2 (\sqrt{v^2 - 2\Delta^*} - v) dv \right]$$

$$= \eta_0 \frac{4S_D^2}{\pi(D+2)D^2} n^{*2} \chi \left[1 + \frac{1}{4} p \left(\Delta^* e^{-(1/2)\Delta^*} K_1\left(\frac{1}{2}\Delta^*\right) - 2e^{-\Delta^*}(1+\Delta^*) \right) \right] \tag{C2}$$

and

$$\bar{\theta} = \frac{3S_D}{2D(D+2)} n^* \chi \left[1 + \frac{1}{2\sqrt{2\pi}} p \int_{\sqrt{2\Delta^*}}^{\infty} v e^{-(1/2)v^2} (v^2 - 1)(\sqrt{v^2 - 2\Delta^*} - v) dv \right]$$

$$= \frac{3S_D}{2D(D+2)} n^* \chi \left[1 + \frac{1}{2} p \left(e^{-\Delta}\left(1 + \Delta - 2\sqrt{\frac{\Delta}{\pi}}(1+\Delta)\right) - (1 - \mathrm{erf}(\sqrt{\Delta})) \right) \right]. \tag{C3}$$

It is also useful to note that

$$\frac{\partial \bar{\gamma}}{\partial \Delta^*} = \frac{4S_D^2 n^{*2} \chi}{D^2(D+2)\pi} \left[\frac{1}{4} p \left(-\frac{1}{2} e^{-(1/2)\Delta^*} \Delta^* \left(K_0\left(\frac{1}{2}\Delta^*\right) + K_2\left(\frac{1}{2}\Delta^*\right) \right) + 2\Delta^* e^{-\Delta^*} \right) \right]$$

$$- \frac{1}{8} p \Delta e^{-(1/2)\Delta} \left(K_1\left(\frac{1}{2}\Delta\right) + K_0\left(\frac{1}{2}\Delta\right) - 4e^{-(1/2)\Delta} \right) \tag{C4}$$

and

$$\frac{\partial \theta}{\partial \Delta^*} = \frac{3S_D}{2D(D+2)} n^* \chi \left[\frac{1}{2} p e^{-\Delta} \left((2\Delta - 1) \sqrt{\frac{\Delta}{\pi}} - \Delta \right) \right]. \tag{C5}$$

2. Dimensionless equations for kinetic parts of the transport coefficients

The kinematic contributions obey

$$\xi_0(D+2)\frac{1}{m}T\frac{\partial \mu^K}{\partial T} + I_{11}^n \mu^K - \xi_0(D+2)\frac{1}{m}T\left(\frac{\partial \ln n\chi_0}{\partial n}\right)\kappa^K = \left(nk_BT\left(\frac{k_BT}{m}\right)\frac{D+2}{2}\right)\Omega_1^n,$$

$$\xi_0(D+2)\frac{1}{m}\left[T\frac{\partial \kappa^K}{\partial T} + \left(T\frac{\partial}{\partial T}\ln \xi_0\right)\kappa^K\right] + I_{11}^T \kappa^K = mn\left(\frac{k_BT}{m}\right)^2\frac{D+2}{2}\left(\Omega_1^T + \frac{n}{T}\frac{k_BT}{m}\frac{D(D+2)}{2}\right),$$

$$\frac{1}{4}\xi_0\frac{D+2}{k_BT}\left[T\frac{\partial}{\partial T}a_2^{(\nabla u)} + 2a_2^{(\nabla u)}\right] + I_{22}^{\nabla u}a_2^{(\nabla u)} = \Omega_2^{\nabla u}, \tag{C6}$$

$$\xi_0\frac{D+2}{m}\left(\frac{2k_BT}{m}\right)T\frac{\partial \eta^K}{\partial T} + I_{00}^{\partial u}\eta^K = mn\left(\frac{k_BT}{m}\right)^2\left[n\left(\frac{k_BT}{m}\right)D(D+2) - 2\sqrt{\frac{D}{D-1}}\Omega_0^{\partial u}\right],$$

where $a_2^{\nabla u} = (\sqrt{m\sigma^2/k_BT})\bar{\gamma}^K$. Introducing the scaled transport coefficients and switching to Δ^* as the independent variable give

$$-\xi_0(D+2)\frac{1}{m}\frac{T}{n}\kappa_0\Delta^*\frac{\partial \bar{\mu}^K}{\partial \Delta^*} + \left[\xi_0(D+2)\frac{1}{m}\frac{3}{2}\kappa_0\frac{T}{n} + I_{11}^n\kappa_0\frac{T}{n}\right]\bar{\mu}^K - \xi_0(D+2)\frac{1}{m}T\left(\frac{\partial \ln n\chi_0}{\partial n}\right)\kappa_0\bar{\kappa}^K = \left(nk_BT\left(\frac{k_BT}{m}\right)\frac{D+2}{2}\right)\Omega_1^n,$$

$$-\xi_0(D+2)\frac{1}{m}\kappa_0\Delta^*\frac{\partial \bar{\kappa}^K}{\partial \Delta^*} + \left[\frac{D+2}{2m}\xi_0 + \frac{D+2}{m}T\frac{\partial}{\partial T}\xi_0 + I_{11}^T\right]\kappa_0\bar{\kappa}^K = mn\left(\frac{k_BT}{m}\right)^2\frac{D+2}{2}\left(\Omega_1^T + \frac{n}{T}\frac{k_BT}{m}\frac{D(D+2)}{2}\right), \tag{C7}$$

$$-\frac{1}{4}\xi_0\frac{D+2}{k_BT}\left[T\sqrt{\frac{m\sigma^2}{k_BT}}\frac{\partial}{\partial T}\bar{\gamma}^K\right] + \left(\frac{1}{4}\xi_0\frac{D+2}{k_BT}\sqrt{\frac{m\sigma^2}{k_BT}} + I_{22}^{\nabla u}\sqrt{\frac{m\sigma^2}{k_BT}}\right)\bar{\gamma}^K = \Omega_2^{\nabla u},$$

$$-\xi_0\frac{D+2}{m}\left(\frac{2k_BT}{m}\right)\eta_0\Delta^*\frac{\partial \bar{\eta}^K}{\partial \Delta^*} + \left[\xi_0\frac{D+2}{m}\left(\frac{2k_BT}{m}\right)\frac{1}{2} + I_{00}^{\partial u}\right]\eta_0\bar{\eta}^K = mn\left(\frac{k_BT}{m}\right)^2\left[n\left(\frac{k_BT}{m}\right)D(D+2) - 2\sqrt{\frac{D}{D-1}}\Omega_0^{\partial u}\right].$$

Next, we introduce dimensionless forms for the Boltzmann integrals

$$\xi_0 = -\frac{Dnk_BT}{2}n\sigma^D\chi\frac{S_D}{2D(D+2)\sqrt{\pi}}\left(\frac{k_BT}{m\sigma^2}\right)^{1/2}I^*_{1,00},$$

$$I^n_{11} = I^T_{11} = I^{TE}_{11}I^*_T,$$

$$I^{\nabla u}_{22} = I^{\nabla uE}_{22}I^*_\gamma,$$

$$I^{\partial u}_{00} = I^{\partial uE}_{00}I^*_\eta,$$

where the elastic contributions are

$$I^{nE}_{11} = I^{TE}_{11} = n^2\sigma^{D-1}S_D\chi\left(\frac{k_BT}{m}\right)^{3/2}\frac{2(D-1)}{\sqrt{\pi}},$$

$$I^{\nabla uE}_{22} = n^2\sigma^{D-1}S_D\chi\left(\frac{k_BT}{m}\right)^{1/2}\frac{(D-1)}{2\sqrt{\pi}},$$

$$I^{\partial uE}_{00} = \chi n^2\sigma^{D-1}S_D\left(\frac{k_BT}{m}\right)^{5/2}\frac{4D}{\sqrt{\pi}},$$

thus giving

$$I^*_{1,00}\Delta^*\frac{\partial\bar{\mu}^K}{\partial\Delta^*} + \left[8(D-1)I^*_T - \frac{3}{2}I^*_{1,00}\right]\bar{\mu}^K$$
$$+ I^*_{1,00}(1 + n\partial_n\chi_0)\bar{\kappa}^K = \frac{16m(D-1)}{k_BT(D+2)D\chi}\Omega^n_1,$$

$$I^*_{1,00}\Delta^*\frac{\partial\bar{\kappa}^K}{\partial\Delta^*} + \left[8(D-1)I^*_T - 2I^*_{1,00} - T\frac{\partial}{\partial T}I^*_{1,00}\right]\bar{\kappa}^K = 8\frac{D-1}{\chi}$$
$$+ 16m\frac{D-1}{k_B(D+2)n\chi D}\Omega^T_1$$

$$I^*_{1,00}\Delta^*\frac{\partial}{\partial\Delta^*}\bar{\gamma}^K + [8(D-1)I^*_\gamma - I^*_{1,00}]\bar{\gamma}^K = \frac{16}{n^2\sigma^D\chi S_D}\sqrt{\pi}\Omega^{\nabla u}_2,$$

$$I^*_{1,00}\Delta^*\frac{\partial\bar{\eta}^K}{\partial\Delta^*} + \left[8DI^*_\eta - \frac{1}{2}I^*_{1,00}\right]\bar{\eta}^K = \frac{8}{\chi}D$$
$$- 8\frac{m}{k_BTn\chi(D+2)}\left[2\sqrt{\frac{D}{D-1}}\Omega^{\partial u}_0\right].$$

Finally, we introduce scaled sources

$$\Omega^{\partial u}_0 = \Omega^{\partial uE}_0\Omega^*_\eta,$$

$$\Omega^{\nabla u}_2 = \chi n^2\sigma^D S_D\Omega^*_\gamma,$$

$$\Omega^T_1 = \Omega^{TE}_1\Omega^*_T,$$

$$\Omega^n_1 = \frac{16m(D-1)}{k_BT(D+2)D\chi}\Omega^*_\mu,$$

with the elastic contributions

$$\Omega^{TE}_1 = n^2\sigma^D\chi S_D\frac{k_BT}{m}\frac{1}{T}\frac{3}{4},$$

$$\Omega^{\partial uE}_1 = -n^2\sigma^D\chi S_D\frac{k_BT}{m}\frac{1}{2}\sqrt{\frac{D-1}{D}},$$

so

$$I^*_{1,00}\Delta^*\frac{\partial\bar{\mu}^K}{\partial\Delta^*} + \left[8(D-1)I^*_T - \frac{3}{2}I^*_{1,00}\right]\bar{\mu}^K + I^*_{1,00}(1 + n\partial_n\chi_0)\bar{\kappa}^K$$
$$= \Omega^*_\mu,$$

$$I^*_{1,00}\Delta^*\frac{\partial\bar{\kappa}^K}{\partial\Delta^*} + \left[8(D-1)I^*_T - 2I^*_{1,00} - T\frac{\partial}{\partial T}I^*_{1,00}\right]\bar{\kappa}^K$$
$$= 8\frac{D-1}{\chi} + 12\frac{(D-1)S_D}{D(D+2)}n^*\Omega^*_T,$$

$$I^*_{1,00}\Delta^*\frac{\partial}{\partial\Delta^*}\bar{\gamma}^K + [8(D-1)I^*_\gamma - I^*_{1,00}]\bar{\gamma}^K = 16\sqrt{\pi}\Omega^*_\gamma,$$

$$I^*_{1,00}\Delta^*\frac{\partial\bar{\eta}^K}{\partial\Delta^*} + \left[8DI^*_\eta - \frac{1}{2}I^*_{1,00}\right]\bar{\eta}^K = \frac{8}{\chi}D + \frac{8S_D}{D+2}n^*\Omega^*_\eta.$$

3. Boltzmann integrals

Within the present approximations, Ref. 25 gives the Boltzmann integrals

$$I^\gamma_{rs} = I^{\gamma E}_{rs}\left[1 + p\int_{\sqrt{2\Delta^*}}^\infty e^{-(1/2)v^2}v\left(\Delta^* S^\gamma_{rs}(v)\right.\right.$$
$$\left.\left. + \frac{1}{4}v(\sqrt{v^2 - 2\Delta} - v)\right)dv\right]$$
$$= I^{\gamma E}_{rs}\left[1 + p\Delta^*\int_{\sqrt{2\Delta^*}}^\infty e^{-(1/2)v^2}vS^\gamma_{rs}(v)dv - \frac{1}{2}pe^{-\Delta^*}(1 + \Delta^*)\right.$$
$$\left. + \frac{1}{4}p\Delta^*e^{-(1/2)\Delta^*}K_1\left(\frac{1}{2}\Delta^*\right)\right],$$

with

$$S^n_{11}(v) = S^T_{11}(v) = \frac{D+8}{16(D-1)}(v^2 - 1),$$

$$S^{\nabla u}_{22}(v) = \frac{1}{64(D-1)}(v^6 - 9v^4 + (8D+49)v^2 - 37 - 8D)$$
$$- \frac{1}{64(D-1)}(v^4 - 6v^2 + 3)\Delta^*,$$

$$S^{\partial u}_{00}(v) = \frac{1}{4D}(v^2 - 1).$$

For the shear viscosity this gives

(C8)

(C9)

(C10)

(C11)

(C12)

(C13)

(C14)

(C15)

$$I_\eta^* \equiv \left(\chi n^2 \sigma^{D-1} S_D \left(\frac{k_B T}{m} \right)^{5/2} \frac{4D}{\sqrt{\pi}} \right)^{-1} I_{00}^{\partial u}$$

$$= 1 + \frac{1}{4D} p\Delta^* \int_{\sqrt{2\Delta^*}}^\infty e^{-(1/2)v^2} v(v^2 - 1)dv - \frac{1}{2}pe^{-\Delta^*}(1 + \Delta^*) + \frac{1}{4}p\Delta^* e^{-(1/2)\Delta^*} K_1\left(\frac{1}{2}\Delta^* \right)$$

$$= 1 + \frac{1}{4D} pe^{-\Delta^*}(2\Delta^{*2} + \Delta^*(1 - 2D) - 2D) + \frac{1}{4}p\Delta^* e^{-(1/2)\Delta^*} K_1\left(\frac{1}{2}\Delta^* \right); \tag{C16}$$

for the bulk viscosity

$$I_\gamma^* \equiv \left(n^2 \sigma^{D-1} S_D \chi \left(\frac{k_B T}{m} \right)^{1/2} \frac{(D-1)}{2\sqrt{\pi}} \right)^{-1} I_{22}^{\nabla u}$$

$$= 1 + \frac{1}{64(D-1)} p\Delta^* \int_{\sqrt{2\Delta^*}}^\infty e^{-(1/2)v^2} v((v^6 - 9v^4 + (8D + 49)v^2 - 37 - 8D) - (v^4 - 6v^2 + 3)\Delta^*)dv - \frac{1}{2}pe^{-\Delta^*}(1 + \Delta^*)$$

$$+ \frac{1}{4}p\Delta^* e^{-(1/2)\Delta^*} K_1\left(\frac{1}{2}\Delta^* \right)$$

$$= 1 + \frac{1}{64(D-1)} pe^{-\Delta^*}(4\Delta^{*4} - 8\Delta^{*3} + (75 + 16D)\Delta^{*2} + (69 - 24D)\Delta^* - 32(D-1)) + \frac{1}{4}p\Delta^* e^{-(1/2)\Delta^*} K_1\left(\frac{1}{2}\Delta^* \right); \tag{C17}$$

and for the density and thermal conductivity

$$I_\kappa^* \equiv \left(n^2 \sigma^{D-1} S_D \chi \left(\frac{k_B T}{m} \right)^{3/2} \frac{2(D-1)}{\sqrt{\pi}} \right)^{-1} I_{11}^{TE}$$

$$= 1 + \frac{D+8}{16(D-1)} p\Delta^* \int_{\sqrt{2\Delta^*}}^\infty e^{-(1/2)v^2} v(v^2 - 1)dv - \frac{1}{2}pe^{-\Delta^*}(1 + \Delta^*) + \frac{1}{4}p\Delta^* e^{-(1/2)\Delta^*} K_1\left(\frac{1}{2}\Delta^* \right)$$

$$= 1 + \frac{1}{16(D-1)} pe^{-\Delta^*}((2D + 16)\Delta^{*2} + (16 - 7D)\Delta^* - 8D + 8) + \frac{1}{4}p\Delta^* e^{-(1/2)\Delta^*} K_1\left(\frac{1}{2}\Delta^* \right). \tag{C18}$$

4. Sources

Reference 25 gives the sources as

$$\Omega_{rs}^\gamma = \Omega_{rs}^{\gamma E} + \chi n^2 \sigma^D S_D \frac{1}{\sqrt{2\pi}} p \int_{\sqrt{2\Delta^*}}^\infty e^{-(1/2)v^2} v T_{rs}^\gamma(v)dv \tag{C19}$$

with

$$T_{11}^n(v) = \frac{1}{2} \frac{\partial \ln n^2 \chi}{\partial n} \left(\frac{k_B T}{m} \right) \frac{1}{4}((v^2 - 3)(\sqrt{v^2 - 2\Delta^*} - v)$$

$$- 2\Delta^*((\sqrt{v^2 - 2\Delta^*} - v) + v)),$$

$$T_{11}^T(v) = \frac{k_B}{16m}((v^4 - 4v^2 + 9)(\sqrt{v^2 - 2\Delta^*} - v)$$

$$- 2\Delta^*((v^2 - 1)(\sqrt{v^2 - 2\Delta^*} - v) + v^3 + 5v)),$$

$$\tag{C20}$$

$$T_{22}^{\nabla u}(v) = \frac{1}{8D}((2\Delta^* + 3 - v^2)(\sqrt{v^2 - 2\Delta^*} - v)$$

$$+ v\Delta^*(v^2 - 1 - \Delta^*)),$$

$$T_{00}^{\partial u}(v) = \frac{1}{2} \sqrt{\frac{D-1}{D}} \left(\frac{k_B T}{m} \right) (v\Delta^* - (\sqrt{v^2 - 2\Delta^*} - v)),$$

so

$$\Omega_1^n = \chi n^2 \sigma^D S_D \frac{1}{\sqrt{2\pi}} p \frac{1}{2} \frac{\partial \ln n^2 \chi}{\partial n} \left(\frac{k_B T}{m} \right)$$

$$\times \int_{\sqrt{2\Delta^*}}^\infty e^{-(1/2)v^2} v \frac{1}{4}((v^2 - 3)(\sqrt{v^2 - 2\Delta^*} - v)$$

$$- 2\Delta^*((\sqrt{v^2 - 2\Delta^*} - v) + v))dv$$

$$= -\chi n^2 \sigma^D S_D \frac{1}{4\sqrt{\pi}} p \frac{\partial \ln n^2 \chi}{\partial n} \left(\frac{k_B T}{m} \right) e^{-\Delta^*} \Delta^{*3/2}$$

$$= \frac{k_B T(D+2)D\chi}{16m(D-1)} \Omega_\mu^* \tag{C21}$$

with

$$\Omega_\mu^* = -\frac{4(D-1)S_D}{\sqrt{\pi}(D+2)D} n^* p(2 + n\partial_n \ln \chi) e^{-\Delta^*} \Delta^{*3/2} \tag{C22}$$

and

$$\Omega_1^{\nabla u} = \chi n^2 \sigma^D S_D \frac{1}{8D\sqrt{2\pi}} p \int_{\sqrt{2\Delta^*}}^{\infty} e^{-(1/2)v^2} v((2\Delta^* + 3 - v^2)$$

$$\times (\sqrt{v^2 - 2\Delta^*} - v) + v\Delta^*(v^2 - 1 - \Delta^*))dv$$

$$= \chi n^2 \sigma^D S_D \Omega_\gamma^* \qquad (C23)$$

with

$$\Omega_\gamma^* = \frac{1}{16\sqrt{\pi}} \frac{1}{D} p\Delta^*(2\sqrt{\Delta^*}(2 + \Delta^*)e^{-\Delta^*}$$

$$- \Delta^* \sqrt{\pi}(1 - \mathrm{erf}(\sqrt{\Delta^*}))). \qquad (C24)$$

For the shear

$$\Omega_1^{\partial u} = - n^2 \sigma^D \chi S_D \frac{k_B T}{m} \frac{1}{2} \sqrt{\frac{D-1}{D}} \Omega^* \qquad (C25)$$

with

$$\Omega^* = 1 - \frac{1}{\sqrt{2\pi}} p \int_{\sqrt{2\Delta^*}}^{\infty} e^{-(1/2)v^2} v(v\Delta^* - (\sqrt{v^2 - 2\Delta^*} - v))dv$$

$$= 1 - \frac{1}{\sqrt{2\pi}} p \left[\sqrt{2\Delta^*}(1 + \Delta^*)e^{-\Delta^*} - \sqrt{\frac{\pi}{2}} e^{-\Delta^*} \right.$$

$$\left. + \sqrt{\frac{\pi}{2}}(1 + \Delta^*)(1 - \mathrm{erf}(\sqrt{\Delta^*})) \right] \qquad (C26)$$

and for the temperature

$$\Omega_1^T = n^2 \sigma^D \chi S_D \frac{k_B T}{m} \frac{1}{T} \frac{3}{4} \Omega^* \qquad (C27)$$

with

$$\Omega^* = 1 + \frac{1}{12} \frac{1}{\sqrt{2\pi}} p \int_{\sqrt{2\Delta^*}}^{\infty} e^{-(1/2)v^2} v((v^4 - 4v^2 + 9)$$

$$\times (\sqrt{v^2 - 2\Delta^*} - v) - 2\Delta^*((v^2 - 1)(\sqrt{v^2 - 2\Delta^*} - v)$$

$$+ v^3 + 5v))$$

$$= 1 + \frac{1}{2} p \left[\left(1 - \frac{1}{3\sqrt{\pi}}(\Delta^* + 2)(2\Delta^* + 3)\sqrt{\Delta^*} \right) e^{-\Delta^*} \right.$$

$$\left. - (1 + \Delta^*)(1 - \mathrm{erf}(\sqrt{\Delta^*})) \right]. \qquad (C28)$$

5. Derivatives

To implement the numerical solution of the Navier-Stokes equations, it is useful to know the derivatives of the Boltzmann integrals and the sources. For convenience these are recorded here for the former,

$$\frac{\partial}{\partial \Delta^*} I_\eta^* = \frac{1}{4} Dp \frac{\partial}{\partial \Delta^*} \left(\frac{1}{D} e^{-\Delta^*}(2\Delta^{*2} + (1 - 2D)\Delta^* - 2D) \right.$$

$$\left. + \Delta^* e^{-(1/2)\Delta^*} K_1 \left(\frac{1}{2}\Delta^* \right) \right)$$

$$= \frac{1}{4} Dp \left(\frac{1}{D} e^{-\Delta^*}(-2\Delta^{*2} + \Delta^*(3 + 2D) + 1) \right.$$

$$- \frac{1}{2}\Delta^* e^{-(1/2)\Delta^*} \left(K_1 \left(\frac{1}{2}\Delta^* \right) + K_0 \left(\frac{1}{2}\Delta^* \right) \right) \right),$$

$$\frac{\partial}{\partial \Delta^*} I_\kappa^* = - \frac{1}{16(D-1)} pe^{-\Delta^*}(2\Delta^{*2}(D+8) - \Delta^*(16 + 11D)$$

$$- D - 8) - \frac{1}{8} p\Delta^* e^{-(1/2)\Delta^*}(D - 1) \left(K_1 \left(\frac{1}{2}\Delta^* \right) \right.$$

$$\left. + K_0 \left(\frac{1}{2}\Delta^* \right) \right),$$

$$\frac{\partial}{\partial \Delta^*} I_\gamma^* = - \frac{1}{64(D-1)} pe^{-\Delta^*}(4\Delta^{*4} - 24\Delta^{*3}$$

$$+ (99 + 16D)\Delta^{*2} - (81 + 56D)\Delta^* - 8D - 37)$$

$$- \frac{1}{8} p\Delta^* e^{-(1/2)\Delta^*} \left(K_1 \left(\frac{1}{2}\Delta^* \right) + K_0 \left(\frac{1}{2}\Delta^* \right) \right), \quad (C29)$$

and for the sources

$$\frac{\partial}{\partial \Delta^*} \Omega_\eta^* = \frac{1}{2} p \left(\mathrm{erf}(\sqrt{\Delta^*}) - 1 + \left(\frac{2}{\sqrt{\pi}}\Delta^{*3/2} - 1 \right) e^{-\Delta^*} \right),$$

$$\frac{\partial}{\partial \Delta^*} \Omega_\kappa^* = \frac{1}{6} p \left(\frac{-3\sqrt{\Delta^*} + 4\Delta^{*3/2} + 4\Delta^{*5/2} - 6\sqrt{\pi}}{2\sqrt{\pi}} e^{-\Delta^*} \right.$$

$$\left. + 3(\mathrm{erf}(\sqrt{\Delta^*}) - 1) \right),$$

$$\frac{\partial}{\partial \Delta^*} \Omega_\mu^* = - p \frac{2}{\sqrt{\pi}} \frac{D-1}{(D+2)D} n^* S_D (2 + n\partial_n \ln \chi)$$

$$\times \sqrt{\Delta^*}(3 - 2\Delta^*)e^{-\Delta^*},$$

$$\frac{\partial}{\partial \Delta^*} \Omega_\gamma^* = \frac{1}{8} \frac{1}{D} p \left((3 + \Delta^* - \Delta^{*2}) \sqrt{\frac{\Delta^*}{\pi}} e^{-\Delta^*} \right.$$

$$\left. - \Delta^*(1 - \mathrm{erf}(\sqrt{\Delta^*})) \right). \qquad (C30)$$

6. Cooling

From Ref. 25, the additional cooling term in the Navier-Stokes equations is

$$(\nabla \cdot \mathbf{u})\xi_1 = \xi_0[f_1] + \xi_1[f_0],$$

$$\xi_0[f_1] = - (\nabla \cdot \mathbf{u})a_2^{\nabla u} n^2 \sigma^D \chi S_D \left(\frac{k_B T}{m\sigma^2} \right)^{1/2} \frac{k_B T}{32\sqrt{\pi}} p$$

$$\times \int_{\sqrt{2\Delta^*}}^{\infty} v e^{-(1/2)v^2} \Delta(v^4 - 6v^2 + 3)dv,$$

$$\xi_1[f_0] = (\nabla \cdot \mathbf{u}) n^2 \sigma^D \chi S_D \frac{k_B T}{2\sqrt{2\pi}D} p \int_{\sqrt{2\Delta^*}}^{\infty} \Delta v^2 e^{-(1/2)v^2} dv,$$

$$\qquad (C31)$$

giving

$$\xi_1 = -p(nk_BT)n^*\chi S_D\Delta^*\left[\frac{1}{32\sqrt{\pi}}(4\Delta^{*2}-4\Delta^*-1)e^{-\Delta^*}\bar{\gamma}^K\right.$$

$$\left.+\frac{1}{4D}\left(2\sqrt{\frac{\Delta^*}{\pi}}e^{-\Delta^*}+(1-\mathrm{erf}(\sqrt{\Delta^*}))\right)\right]. \qquad (C32)$$

[1] K. S. Suslick, Science **247**, 1439 (1990).

[2] D. Lohse, Phys. Today **56**(2), 36 (2004).

[3] M. P. Brenner, S. Higenfeldt, and D. Lohse, Rev. Mod. Phys. **74**, 425 (2002).

[4] C. C. Wu and P. H. Roberts, Phys. Rev. Lett. **70**, 3424 (1993).

[5] W. Moss, D. B. Clarke, J. W. White, and D. A. Young, Phys. Fluids **6**, 2979 (1994).

[6] L. Kondic, J. I. Gersten, and C. Yuan, Phys. Rev. E **52**, 4976 (1995).

[7] V. Q. Vuong and A. J. Szeri, Phys. Fluids **8**, 2354 (1996).

[8] L. Yuan, H. Y. Cheng, M.-C. Chu, and P. T. Leung, Phys. Rev. E **57**, 4265 (1998).

[9] Y. An and C. F. Ying, Phys. Rev. E **71**, 036308 (2005).

[10] K. Yasui, Phys. Rev. E **56**, 6750 (1997).

[11] L. Frommhold and A. A. Atchley, Phys. Rev. Lett. **73**, 2883 (1994).

[12] S. Sivasubramanian, A. Widom, and Y. N. Srivastava, e-print cond-mat/0207465.

[13] S. Hilgenfeldt, S. Grossman, and D. Lohse, Phys. Fluids **11**, 1318 (1999).

[14] L. Frommhold, Phys. Rev. E **58**, 1899 (1998).

[15] Y. T. Didenko and K. Suslick, Nature (London) **418**, 394 (2002).

[16] R. Toegel, S. Higenfeldt, and D. Lohse, Phys. Rev. Lett. **88**, 034301 (2002).

[17] H. M. Jaeger, S. R. Nagel, and R. P. Behringer, Phys. Today **49**(4), 32 (1996).

[18] *Granular Gases*, Lecture Notes in Physics Vol. 564, edited by T. Pöschel and S. Luding (Springer, Berlin, 2000).

[19] *Granular Gas Dynamics*, Lecture Notes in Physics Vol. 624, edited by T. Pöschel and N. Brilliantov (Springer, Berlin, 2003).

[20] P. Gaspard and J. Lutsko, Phys. Rev. E **70**, 026306 (2004).

[21] J. A. McLennan, *Introduction to Nonequilibrium Statistical Mechanics* (Prentice-Hall, Englewood Cliffs, NJ, 1989).

[22] J.-P. Hansen and I. McDonald, *Theory of Simple Liquids* (Academic, San Diego, CA, 1986).

[23] J. F. Lutsko, J. Chem. Phys. **120**, 6325 (2004).

[24] V. Garzó and J. W. Dufty, Phys. Rev. E **59**, 5895 (1999).

[25] J. F. Lutsko, Phys. Rev. E **72**, 021306 (2005).

[26] J. A. Barker and D. Hendersen, Rev. Mod. Phys. **48**, 587 (1976).

[27] G. A. Bird, *Molecular Gas Dynamics and Direct Simulation of Gas Flows* (Clarendon, Oxford, 1994).

[28] J. M. Montanero and A. Santos, Phys. Rev. E **54**, 438 (1996).

[29] D. A. McQuarry and J. D. Simon, *Physical Chemistry: A Molecular Approach* (University Science Books, Sausalito, CA, 1997).